SPE 37445

Design of Smart Wellhead Controllers for Optimal Fluid Injection Policy and Producibility in Petroleum Reservoirs: A Neural Network-Model Predictive Approach

Masoud Nikravesh, Lawrence Berkeley National Laboratory, SPE, Masoud Soroush, Drexel University, R. M. Johnston, CalResources, LLC., SPE, T. W. Patzek, University of California, SPE

This paper was prepared for presentation at the 1997 SPE Production Operations Symposium, 9-11 March 1997, Oklahoma City, Oklahoma, U.S.A..

Abstract

In this paper we present the second generation of "smart" controllers for fluid injection and predictive techniques for developing optimal fluid injection policy. A neural network model is used to optimize the oil field management in terms of fluid injection and oil recovery. We illustrate performance of the neural network for model identification and control purposes. In particular, the neural network models are used to control and predict the behavior of individual injectors in CalResources' Phase III steam drive pilot in the South Belridge Diatomite, CA, under different injection policies.

Introduction

In the last few years, we have carried out several projects on waterflood and steamdrive in tight, fractured reservoirs, and have analyzed the dynamics of these processes. In these projects, many injection wells have undergone unwanted fracture extensions and linkage with adjacent producers through the damaged formation. We have learned that an important factor causing fracture extension has been the aggressive action of Proportional-Integral-Derivative (PID) controllers during injector start-up periods, or when the injectors are operated near fracturing pressure. This aggressive action has resulted in reservoir and well damage, injectant recirculation, and irreversibly lost oil production. To prevent such unwanted fracture extensions and formation damage, and to optimize fluid injection, an optimal injection policy (i.e., the schedule of injection rates and pressures chosen to produce a field) is required.

An optimal fluid injection policy maximizes oil recovery per barrel of injected fluid while minimizing formation damage and maintaining reservoir pressure. There are two approaches to prevent the formation damage. The first approach is to tune the PID controller frequently to maintain satisfactory performance. Because the behavior of oil reservoirs under fluid injection is often complex, nonlinear and non-stationary, the controller retuning is time consuming and requires a combination of operational experience, trial-and-error procedures and precise knowledge about the reservoir dynamics. In short, tuning a PID controller in these processes can be quite challenging and often impractical. The second approach is to use a robust, model-based, nonlinear controller. In recent work [1-2], we showed that neural networks are capable of making accurate predictions, even if all mechanisms affecting injection, production, and formation damage are not elucidated. Therefore,

neural networks can be used to design model-based controllers that are capable of providing high quality control in the reservoirs. In addition, we showed that neural network model-based control strategies are robust enough to perform well over a wide range of operating conditions and that they are much easier to design and implement than classical PID control. Despite the incompletely-understood reservoir dynamics, this approach is preferred and is the subject of this paper.

Neural Network

During the past several years, neural networks have received considerable attention. Today, they are used for modeling a variety of processes. In our view, neural networks are attractive because: (1) it can be trained easily with historical data, (2) it has ability to infer general rules and extract typical patterns from specific examples, and (3) it recognizes input-output mapping parameters from complex multi-dimensional data. From a control theory viewpoint, the ability of neural networks to model nonlinear systems is perhaps the most significant feature.

Fig. 1 shows the structure of a conventional neural network model. The typical neural network has an input layer (layer in which input data are presented to the network), an output layer (layer in which output data are presented to the network, network prediction), and at least one hidden layer.

Several techniques have been proposed for training the neural network models. The most common technique is the backpropagation [3-5] approach. The objective of the learning process is to minimize the global error in the output nodes by adjusting the weights. This minimization is usually set up as an optimization problem. Here, we use the Levenberg-Marquardt algorithm, which is faster and more robust than the conventional algorithms, but it requires more memory.

Field Application

The CalResources Phase III Steam Drive Pilot is located in Section 33 of the South Belridge Diatomite, Kern County, California (**Fig. 2**). This pilot has 12 steam injectors, 9 producers, and 13 vertical observation wells. Nominally, the wells are staggered on a 5/8-acre spacing. The steam injection wellhead pressures and rates in all the Phase III pilot injectors have been acquired at 30-second intervals and transmitted over Internet to Cal. The temperature logs have been acquired once a month.

The central pilot injector, 553AR, is surrounded by four observation wells (753LO7 and 753PO1 on the east side, and 753LO5 and 753LO6 on the west side) and, therefore, its performance can be verified perhaps better than those of the other 11 injectors. **Figs. 3 and 4** show the maximum, average and minimum injection pressures and rates in 553AR, averaged over 24-hour periods through January 7, 1997. If these three quantities overlap with each other, then both the injection pressure and rate are controlled well. Fig. 3 shows that the wellhead injection pressure, which is the primary controlled variable, remains essentially constant over each 24-hour period, with the exception of down-times and occasional upsets. This pressure has been increased in two ramps up to 664 psig. On the other hand, Fig. 4 demonstrates that the injection rate, which is the manipulated variable when it falls below the preset maximum, is controlled less well and experiences many spikes which double or triple its average values. **Fig. 5** shows this phenomenon in more detail over a 15-day period of steam injection. The occasional pressure upsets cause the rate to jump abruptly. These rate spikes are then choked by closing the steam injection valve at the wellhead and decreasing the injection pressure somewhat. In between these upsets, the pressure is controlled extremely well. The cumulative steam in 553AR has been some 57,000 barrels CWE over the first 467 days of injection, **Fig. 6**. This volume is identical to that injected over the same period of time in the prior Phase II steam drive pilot injector, IN2L, which was also completed across the bottom half of the diatomite column [6, 7]. Note, however, that at the end of the initial 467 days of injection, the steam injection rates (here slopes) in both pilots were very different. By that time, IN2L had linked to a close producer, 543P-29, 40 feet west of it [6]. No such linkage occurred between 553AR and its adjacent producers 553M1 and 553R1.

The second steam injector considered here is 563LR. Its average injection pressure, **Fig.7,** and rate, **Fig. 8,** are controlled less well than those in 553AR. The cumulative steam injected after 400 days on injection and the injection rate both similar to those in IN2L, **Fig. 9**.

The temperature response to steam injection in 553AR is shown in **Figs. 10-11** to the west of the hydrofracture planes, and in **Figs. 12-13** to the east of them. The two east observation wells (PO-1 and LO-7) are almost vertical across the diatomite column, and are nominally 25 feet E-SE from the upper hydrofracture plane, and 40 feet E-SE from the lower one. The west observation wells are also vertical and are nominally 10 ft (LO-5) and 25 feet (LO-6) W-NW from the upper hydrofracture plane, and 30 feet and 15 feet W-NW from the lower hydrofracture plane, respectively. If the conductive heating from a slowly moving heat front dominates, and the hydraulic diffusivities are equal on both sides of the hydrofractures in 553AR, then one expects the observation wells to respond in proportion to the east/west injection $\times$ distance $/\sqrt{\text{time}}$. Therefore, one expects LO-7, PO-1 and LO-6 to respond similarly across the upper injection interval. They do not. For example, about six times more heat goes towards LO-6 than LO-7. If one then compares PO-1 after 569 days with in LO-6 after 100 days, then somewhat more heat is flowing towards PO-1 than LO-6. A similar comparison of LO-7 and LO-6 reveals the same behavior. Hence, from Figs. 10-13 it follows that the square-root-of-time scaling is approximately correct for the lower hydrofracture, but the upper one requires a more sophisticated analysis, such as the one in Refs. [6, 7].

The first discernible heating to the east of 553AR occurs after 100 days of steam injection. Then, the heating progresses in proportion to the square root of time until 200-300 days on injection. Later, the rate of heating slows down visibly, probably due to a rearrangement of steam injection westward. To the west of the hydrofracture planes in 553AR, the response in LO-7 is mostly through conductive heating and mostly at the boundary of the L and K cycles. This response accelerates, however, in the M-cycle after 300 days on injection. A strong temperature response is also evident in PO-1 in the M-cycle. Unfortunately, in this well, the temperature logs extended to the M-cycle only after 500 days on injection.

Model Identification for the CalResources Steam Injectors

Historical data from two steam injectors in the Phase III pilot have been used to develop their neural network (NN) models. The inputs to each model are flow rates and wellhead pressures in 30-second intervals.

The NN model has ten input nodes, three hidden nodes (with a nonlinear transfer function), and one output node (with a nonlinear transfer function). The inputs include 1 current value and 4 previous values of the injection pressure and flow rate for a given well. The output is a prediction of the injection flow rate one time interval into the future. The input and output data are scaled uniformly between 0 and 1. **Figs. 14** and **15** show excellent performance of the network models.

In addition, we developed a NN model for prediction of the injection pressure. The NN model has ten input nodes, five hidden nodes (with a nonlinear transfer function), and one output node (with a nonlinear transfer function). The inputs include 1 current value and 4 previous values of the injection pressure and flow rate for a given well. The output is a prediction of the injection pressure one time interval into the future. The input and output data are scaled uniformly between 0 and 1. **Figs. 16** and **17** show excellent performance of the network models.

To predict the outputs more than one time step into the future, iteration through the neural network is required. **Fig. 18** shows that the performance of the network is seriously affected by iteration. However, this model is effective and has good performance for up to 20 steps into the future (**Fig. 19)**. Hence, this model can be used without any further modification for Neuro-Geometric control [1] or Dynamic Neural Network control (DNNC) [9, 10], since in this case we only need one-step prediction. For model-based strategies with more than one step, usually we need less than 10 iterations. Therefore, for Long-Prediction-Horizon Model Predictive control purposes, this model should also be sufficient.

To study different scenarios of injection policies however, we need more iterations. Unfortunately, conventional neural networks are not stable once they are subjected to long-term prediction through iteration. In this study, an alternative model proposed in Ref. [9, 10] is used. In this model, part of the information from the input layer is presented into the output layer. The effect of this additional connection is to filter the prediction from the hidden layer. This prevents noise from propagating further into the network predictions. **Figs. 20** and **21** show the structure and performance of the new network model. However, further study is needed to better understand the properties of this new

model.

Controller Design

Injector Model: The injector model is developed based on historical data. This model is assumed to represent a real injector. The model is of the form

$$P(k+1) = h\{F(k-4), \ldots, F(k), P(k-4), \ldots, P(k)\} \quad (1)$$

where P is the wellhead pressure, F is the flow rate of injected fluid, and h{., ..., .} is a smooth nonlinear function. The preceding model can easily be written in state-space [1] form by setting

$$\begin{aligned} x(k) &= [F(k-4), \ldots, F(k-1), P(k-4), \ldots, P(k-1), P(k)]^T \\ u(k) &= F(k) \\ y(k) &= P(k) \end{aligned} \quad (2)$$

The model of (1) can be rewritten in the following form:

$$\begin{aligned} x(k+1) &= f\{x(k)\} + g\{x(k), u(k)\}, \\ y(k) &= x_9(k) \end{aligned} \quad (3)$$

with

$$f\{x(k)\} = [x_2(k) \ldots x_4(k)\ 0\ x_6(k) \ldots x_9(k)\ 0]^T$$

$$g\{x(k), u(k)\} = [0\ 0\ 0\ u(k)\ 0\ 0\ 0\ 0\ h\{x(k), u(k)\}]^T \quad (4)$$

Once the injector model has been transformed into the state space form of Equation (3), the approach described in Refs. [1, 9] can be used to design a model-based controller and to analyze the setpoint tracking performance of the neural network controller.

Nonlinear Controller: A neural network model can be used for controller synthesis directly or indirectly. In this study, an indirect method is used, i.e., the inverse of the process model at each sampling time is calculated numerically. We consider an objective function of the form:

$$E(k) = [\nu(k) - h\{., \ldots, .\}]^2 \quad (5)$$

where ν(k) is a reference value given by[10, 11]:

$$\begin{aligned} \nu(k) &= \nu(k-1) + (1-\varphi)\,[y^{set}(k) - d(k) - \nu(k-1)] \\ \nu(0) &= y(0) \\ d(k) &= y_m(k) - y(k) \end{aligned} \quad (6)$$

where φ is an adjustable parameter such that $0 < \varphi < 1$ and y_m is the measured value for controlled variable. The smaller the parameter φ, the faster the closed-loop response.

The Newton-Raphson method is used for the numerical inversion, as in [11, 12]. The following equations are used in this method at each iteration j to calculated the controller action.

$$u(k)^{[j]} = u(k)^{[j-1]} - \frac{E(k)^{[j-1]}}{\left[\partial E(k)^{[j-1]} \Big/ \partial u(k)^{[j-1]}\right]} \quad (7)$$

with the initial guess for u(k) as follows,

$$u(k)^{[0]} = u(k-1). \quad (8)$$

Details of the Jacobian, $\left[\partial E(k)^{[j-1]} \Big/ \partial u(k)^{[j-1]}\right]$, calculation have been presented in Refs. [1, 11, 13, 14].

Controller Implementation

To illustrate the performance of the Neuro-Model Predictive Controller (NMPC), the developed controller model is applied to control the Phase III steam injectors. The open-loop step responses for a series of step changes in injection flow rate is shown in **Fig. 22**. It is seen that the model is highly nonlinear. NMPC was tuned with a filter constant value of φ=0.90. **Fig. 23** shows the setpoint tracking performance of NMPC. The controller performs very well in tracking the setpoint. In addition, Fig. 23 shows the setpoint tracking performance of NMPC with different filter constant φ. Increasing φ will result in the slower but smoother response. Decreasing φ will result in a faster but more oscillatory response.

Conclusions

We presented a detailed case study in which Neuro-Model Predictive Control (NMPC) strategy was applied to a fluid injector. We showed that the NMPC strategy is robust enough to perform well over a wide range of operating conditions. The performance of the NMPC was tested by applying it off-line to several steam injectors at CalResources, LLC. Currently, we are developing a computer interface to implement the NMPC on-line.

Despite our incomplete knowledge, neural network models have been able to predict the complex behavior of steam injectors. The conventional neural network models are sufficiently good for a short term prediction. Unfortunately, these models are not stable, once they are subjected to long-term prediction through iteration. In this study, a special network model was used. In this model, part of the information from the input layer is presented to the output layer. This prevents the noise from propagating further into the network prediction. It has been shown that the model can stabilize the propagation of the noise and therefore has excellent performance for long term prediction In this study, an accurate model for short- and long-term prediction of steam flood injector was identified. However, to understand the full potential of the current model further investigation is required.

Acknowledgments

We thank CalResources LLC for providing the Phase III steam drive pilot steam injection data, and temperature logs. This work was supported partially by the Office of Laboratory Technology Applications, Office of Energy Research of the U.S. Department of Energy under contract No. DE-ACO3-76FS00098 (ACTI) to the Ernest Orlando Lawrence Berkeley National Laboratory of the University of California. Partial support was also provided by CalResources LLC, through U.C. Oil Consortium of the University of California at Berkeley.

References

1. Nikravesh, M., Soroush, M., R. M. Johnston, and Patzek, T. W., “Design of Smart Wellhead controllers for Optimal Fluid Injection Policy and Producibilty in Petroleum Reservoirs: A Neurao-Geometric Approach,” SPE 37557, 1997 International Thermal Operations and Heavy Oil Symposium, Bakersfield, California.
2. Nikravesh, M., Kovscek, A. R., Patzek, T. W., and Johnston, R. M., "Prediction of Formation Damage During Fluid Injection into Fractured, Low Permeability Reservoirs via Neural Networks," SPE 31103, presented at SPE Formation Damage Symposium, Lafayette, LA, 1996.
3. Rumelhart, D. E., Hinton, G. E., and Williams, R. J., "Learning Internal Representations by Error Propagation," in *Parallel Data Processing,* D. Rumelhart and J. McClelland, Editor, MIT Press, Cambridge, MA, 1986, 318-362.
4. Widrow, B. and Lehr, M. A., "30 Years of Adaptive Neural Networks: Perceptron, Madaline, and Backpropagation," *Proceedings of the IEEE*, **78**(9), 1990, 1414-1442.
5. Hecht-Nielsen, R., "Theory of Backpropagation Neural Networks," presented at IEEE Proc., Int. Conf. Neural Network, Washington, DC, 1989.
6. Kovscek, A. R., Johnston, R. M., and Patzek, T.W., “Interpretation of Hydrofracture Geometry Using Temperature Transients I: Model Formulation and Verification,” *In Situ*, **20** 3, 1996, 221-250.
7. Kovscek, A. R., Johnston, R. M., and Patzek, T. W., “Interpretation of Hydrofracture Geometry Using Temperature Transients II: Asymmetric Hydrofractures,” *In Situ*, **20** 3, 1996, 251-289.
8. Soroush, M., Nikravesh, M., "Shortest-Prediction-Horizon Nonlinear Model Predictive Control," 13th World Congress, International Federation of Automatic Control, IFAC, San Francisco, California, June 30-July 5, 1996.
9. Nikravesh, M., Farell, A. E., Stanford, T. G., “Optimal DNNC for Nonlinear Systems Based on Stability Analysis,” *Chemical Engineering Journal*, to be published in 1997.
10. Nikravesh, M., “Dynamic Neural Network Control (DNNC): Smart Wellhead Controller for Water and Steam Injectors,” SPE 38275, 1997 SPE Western Regional Meeting, Long Beach, California.
11. Nahas, E., Henson, M., Seborg, D., “ Non-Linear Internal Model Control Strategy for Neural Network Models,” *Comp. and Chem. Eng.*, **16** (12), 1992, 1039
12. Pschogios, C. D., Ungar, L. H., “Direct and indirect model based control using Artificial

Neural Network," *Ind. Eng. Chem. Res.*, **30**, 1991, 2564.
13. Azimi, M. R., and R. J. Liou, "Fast Learning Process of Multilayer Neural Networks Using Recursive Least Squares Method," *IEEE Transaction on Signal Processing*, **40,** 1992, 446-450.
14. Nikravesh, M., Farell, A.E., and Stanford, T.G., "Model Identification of Nonlinear Time Variant Processes Via Artificial Neural Networks," *J. of Computers and Chemical Engineering*, **20** (11), 1996.

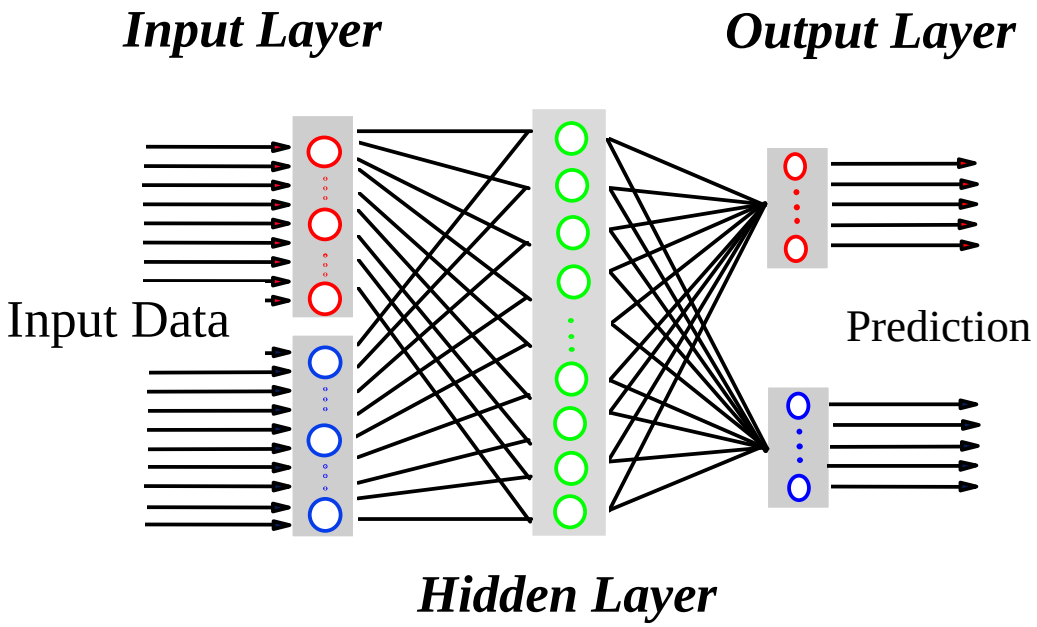

Figure 1. Conventional neural network model

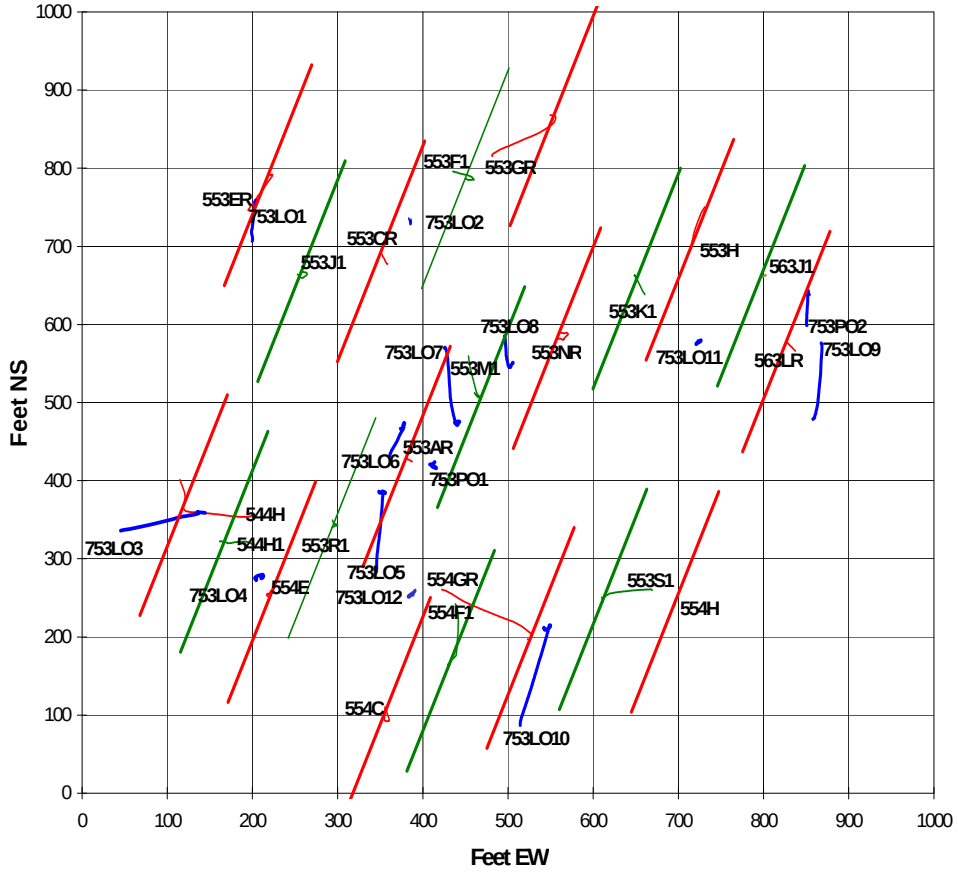

Fig. 2. The CalResources Phase III Steam Drive Pilot in the South Belridge Diatomite.

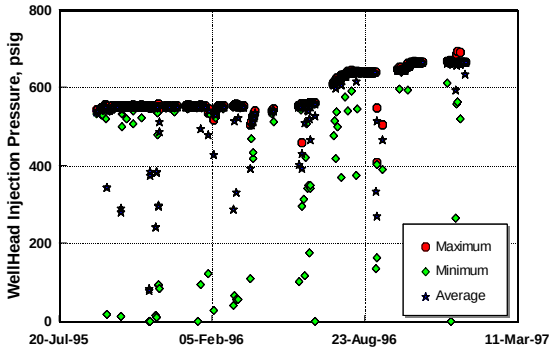

Fig. 3. 24-hour averages of 30-second measurements of WH steam pressure in 553AR. This plot represents 880,000 data points.

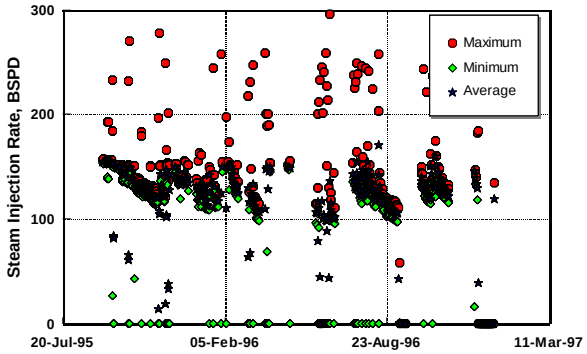

Fig. 4. 24-hour averages of steam injection rate in 553AR. The average rate is usually close to the minimum rate, indicating sporadic rate spikes which double the average injection rate.

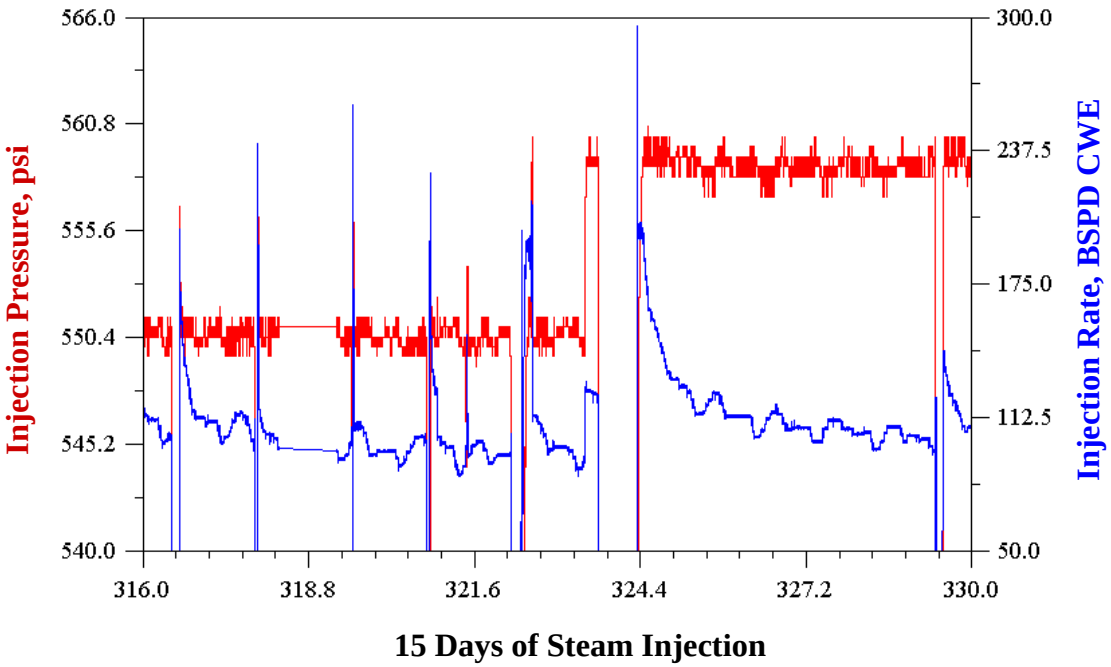

Fig. 5. 30-second measurements of injection rate and wellhead pressure in 553AR. Note that sporadic pressure upsets cause injection rate spikes up to three-times the average.

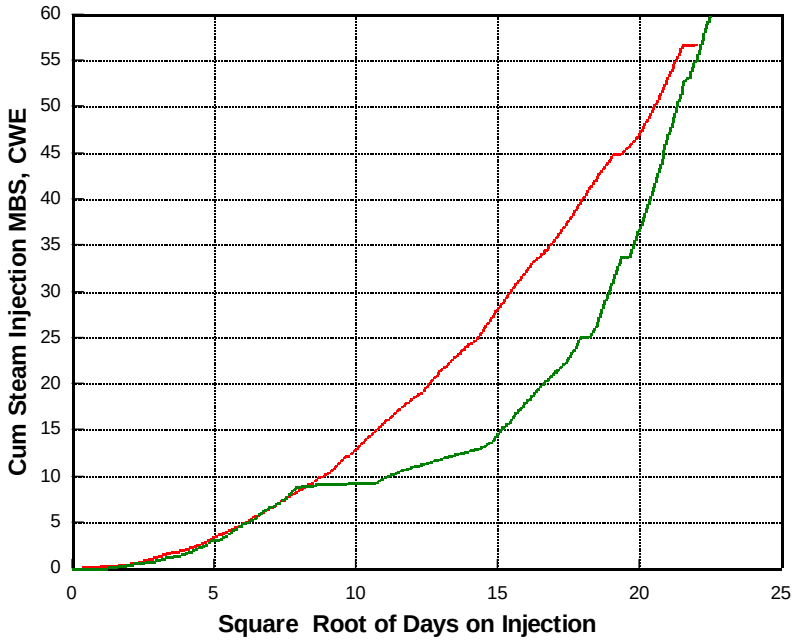

Fig. 6. The cumulative steam injection in 553AR-33 (upper curve) compared with that in IN2L-29 in the Phase II Pilot. Note that after 460 days on injection, both cumulatives are the same, but IN2L injects at a much higher rate because it linked with the nearby producer, 543P-29.

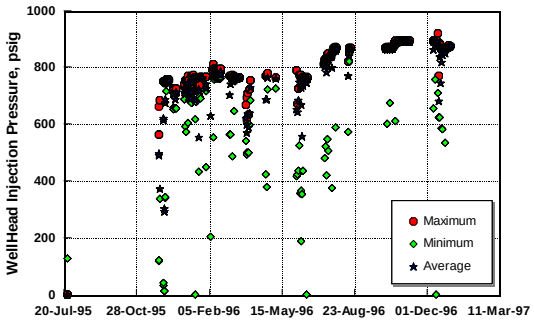

Fig. 7. 24-hour averages of 30-second measurements of WH steam pressure in 563LR. This plot represents 670,000 data points.

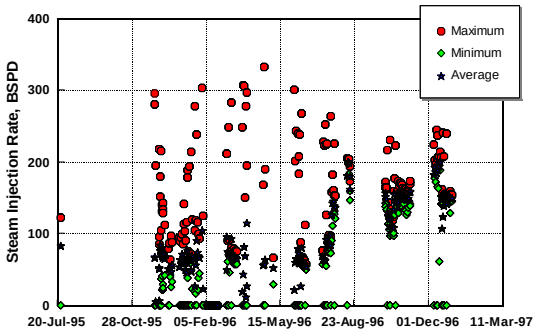

Fig. 8. 24-hour averages of steam injection rate in 563LR. The average rate is usually close to the minimum rate, indicating sporadic rate spikes which triple the average injection rate.

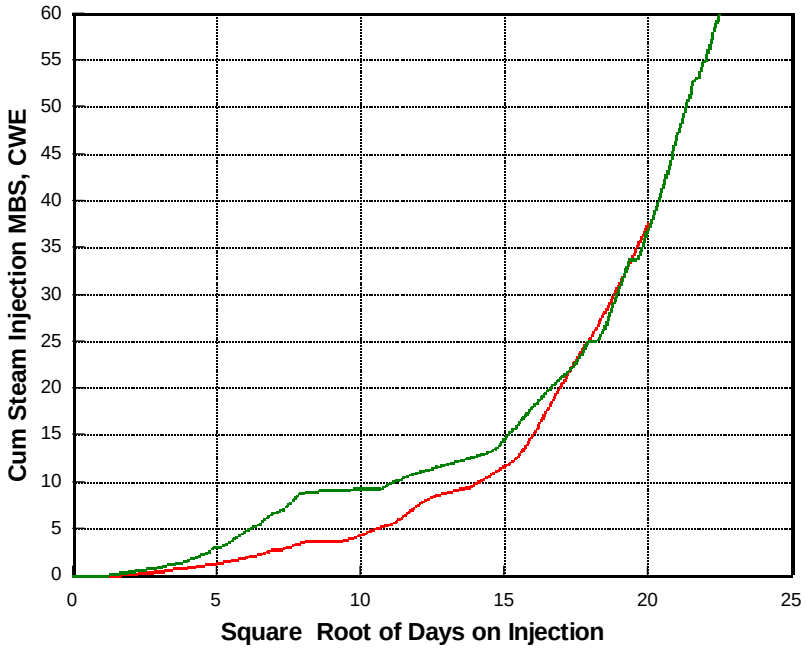

Fig. 9. The cumulative steam injection in 563LR-33 (lower curve) compared with that in IN2L-29 in the Phase II Pilot. Note that after 400 days on injection, both cumulatives are the same, and both wells inject at roughly the same rate.

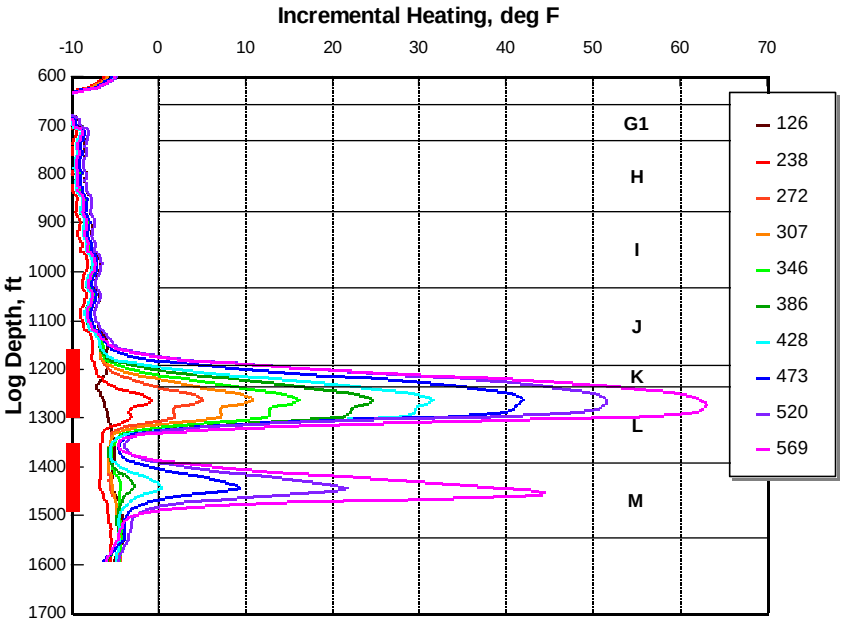

Fig. 10. The incremental rock heating near LO-7, 24-40 ft east of 553AR. The temperature profiles are drawn in equal increments of the square root of time. A uniform spacing between these profiles indicates conduction-dominated heating. Note that the logs are miscalibrated, relative to the first one, by up to 10^0F.

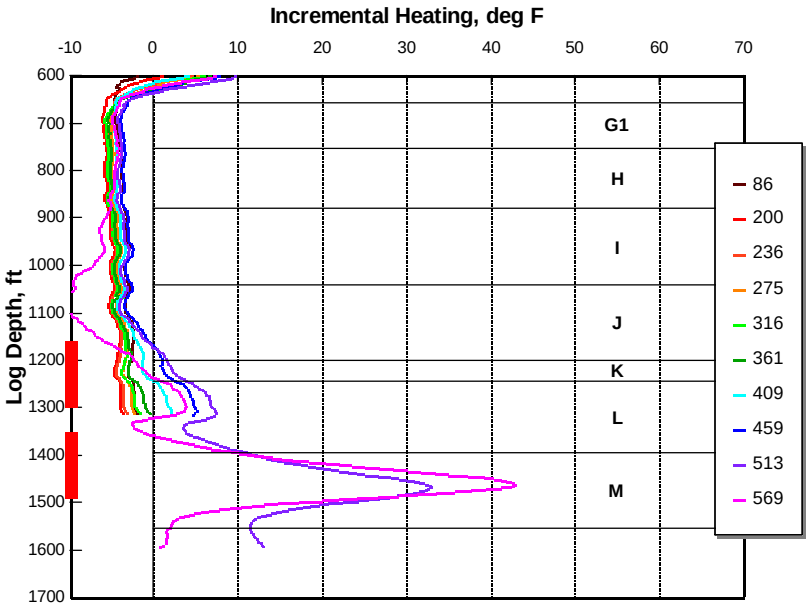

Fig. 11. The incremental rock heating near PO-1, 25-40 ft east of 553AR-33. The temperature profiles are drawn in equal increments of the square root of time. Only the two latest profiles extend to the M-cycle Uniform heating by conduction is evident in the L cycle. Note that the J, K and L cycles appear to have cooled by up to 10^0F at 569 days, while the M-cycle heated up.

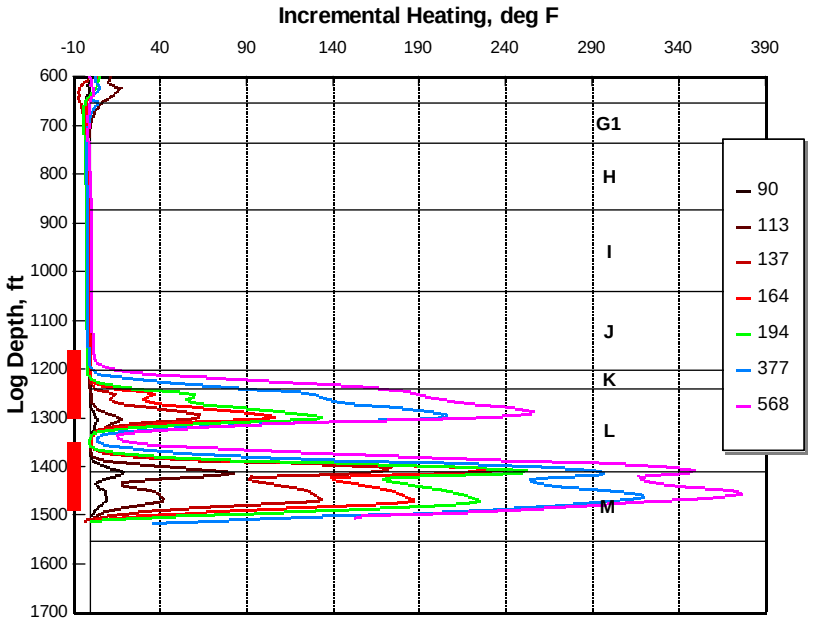

Fig. 12. The incremental rock heating near LO-5, 10-30 ft west of the hydrofracture planes in 553AR-33. The temperature profiles are drawn in equal increments of the square root of time. Note that the rate of heating slowed markedly between 194, 377 and 568 days (the last three profiles). Also note that the magnitude of response is 380^0F.

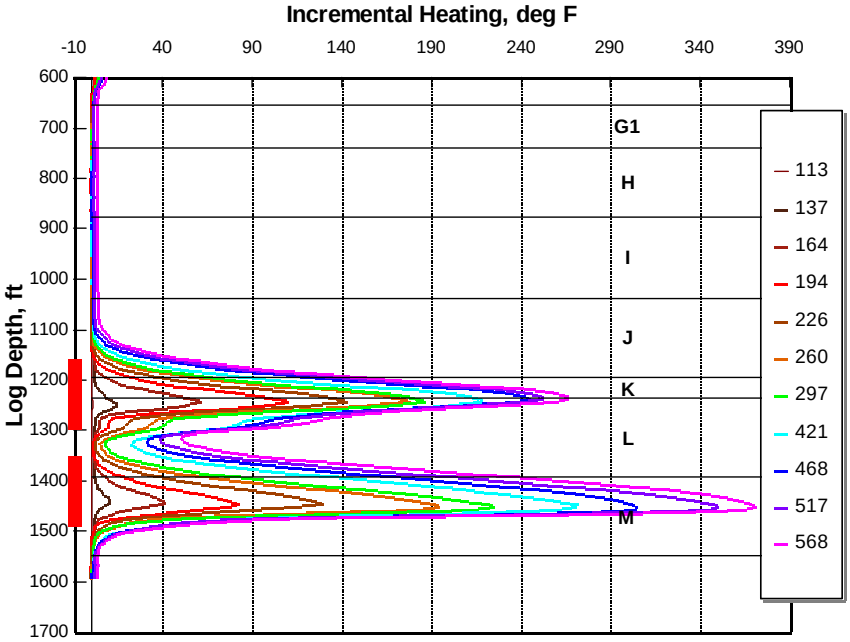

Fig. 13. The incremental rock heating at LO-6, 15-25 ft west of the hydrofracture planes in 553AR-33. The temperature profiles are drawn in equal increments of the square root of time. Note that the rate of heating slows markedly between 297and 568 days of injection (the last four profiles).

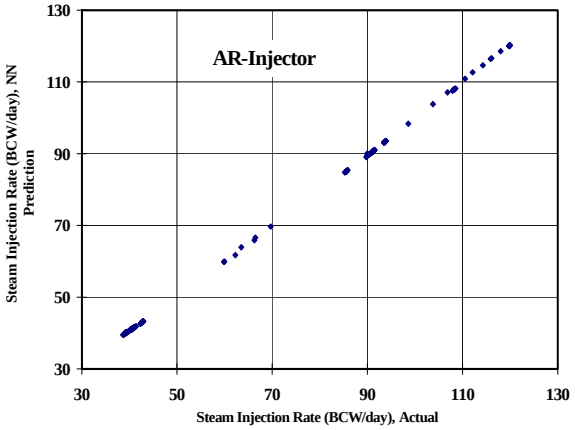

Fig. 14. Neural network prediction for injection rate, Injector AR.

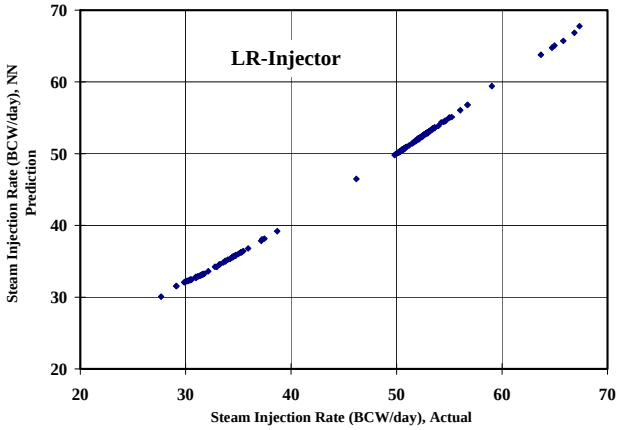

Fig 15. Neural network prediction for injection rate, Injector LR.

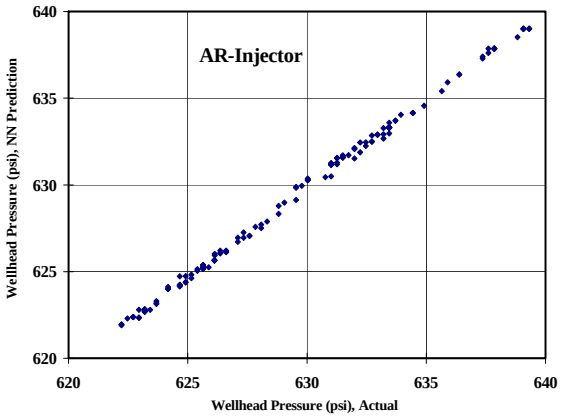

Fig 16. Neural network prediction for wellhead pressure, Injector AR.

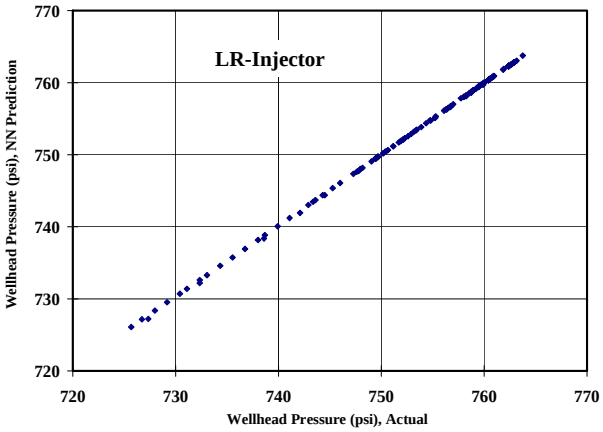

Fig 17. Neural network prediction for wellhead pressure, Injector LR.

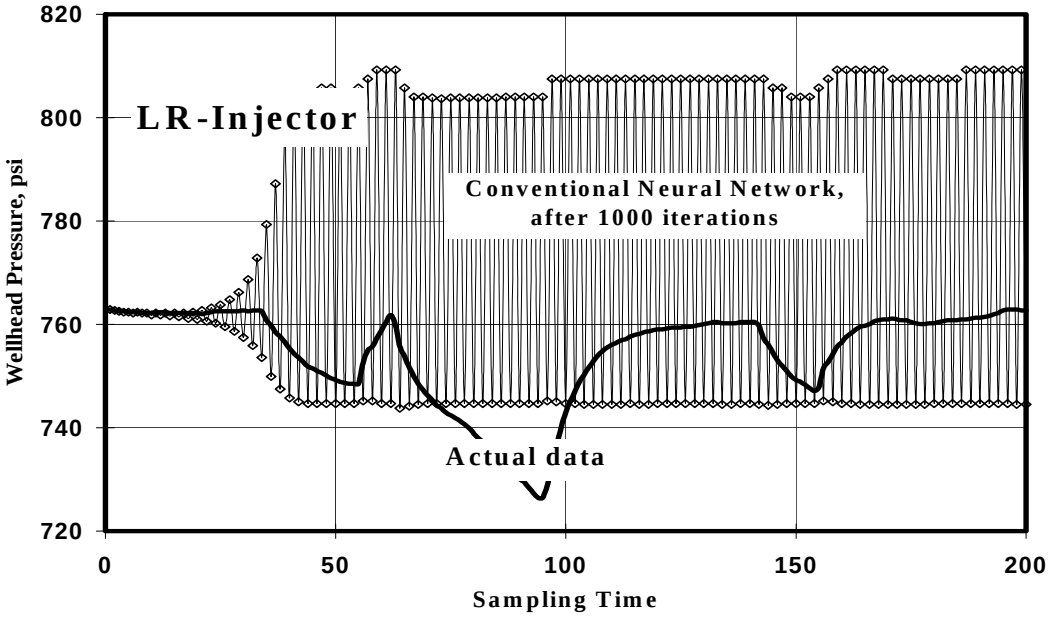

Fig. 18. Performance of conventional neural network after 1000 iterations.

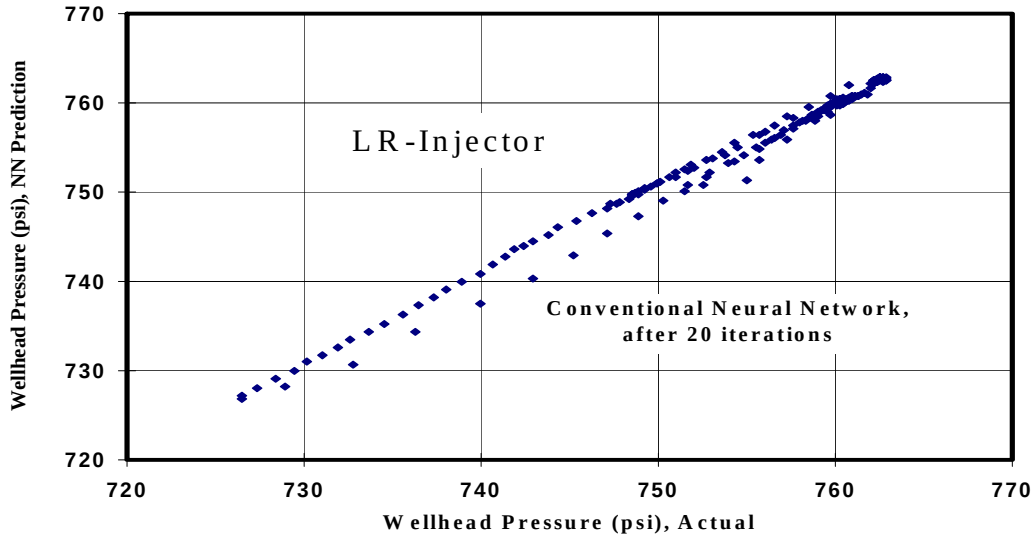

Fig. 19. Performance of conventional neural network up to 20 iterations.

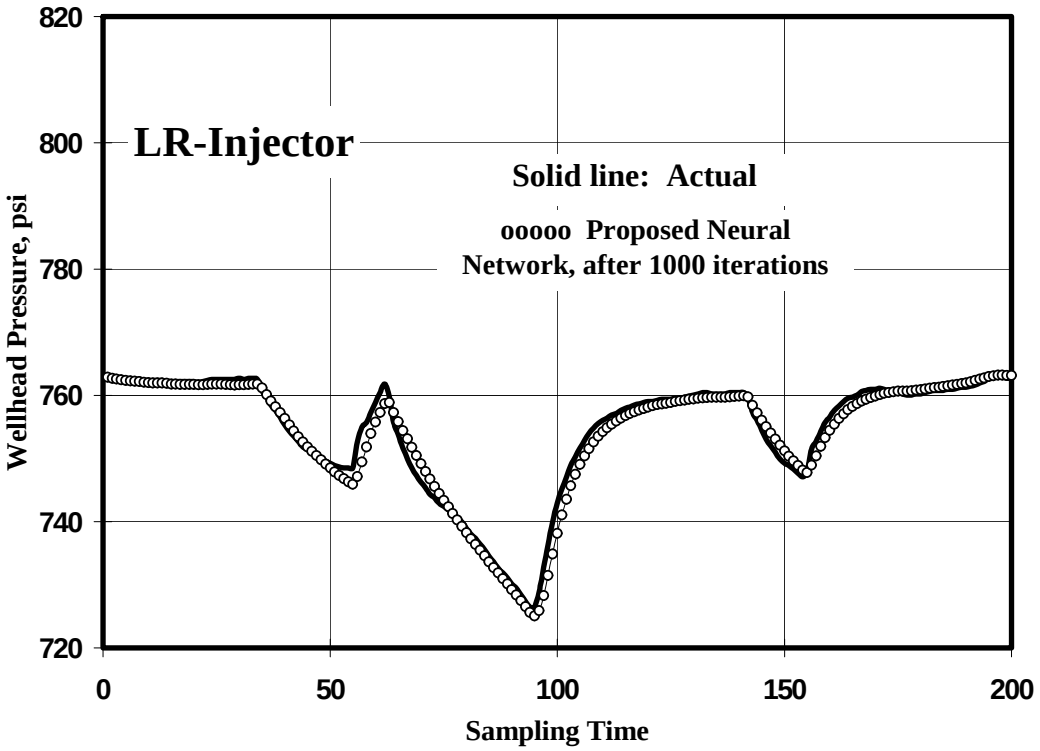

Fig. 20.a. Performance of proposed neural network after 1000 iterations.

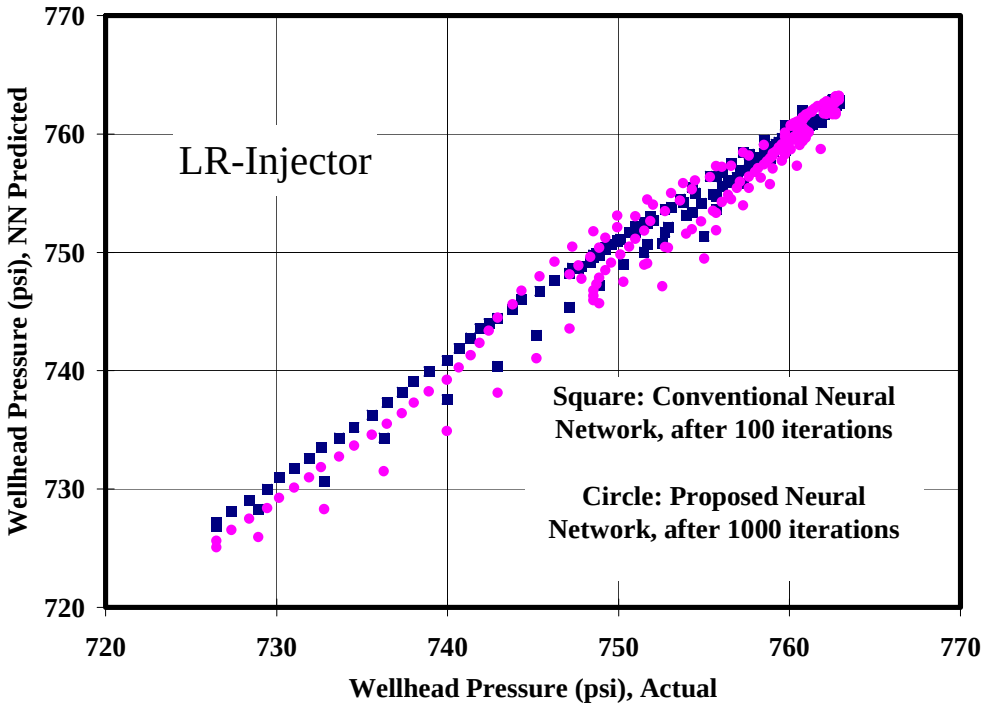

Fig. 20.b. Performance of conventional neural network after 100 iterations and proposed neural network after 1000 iterations.

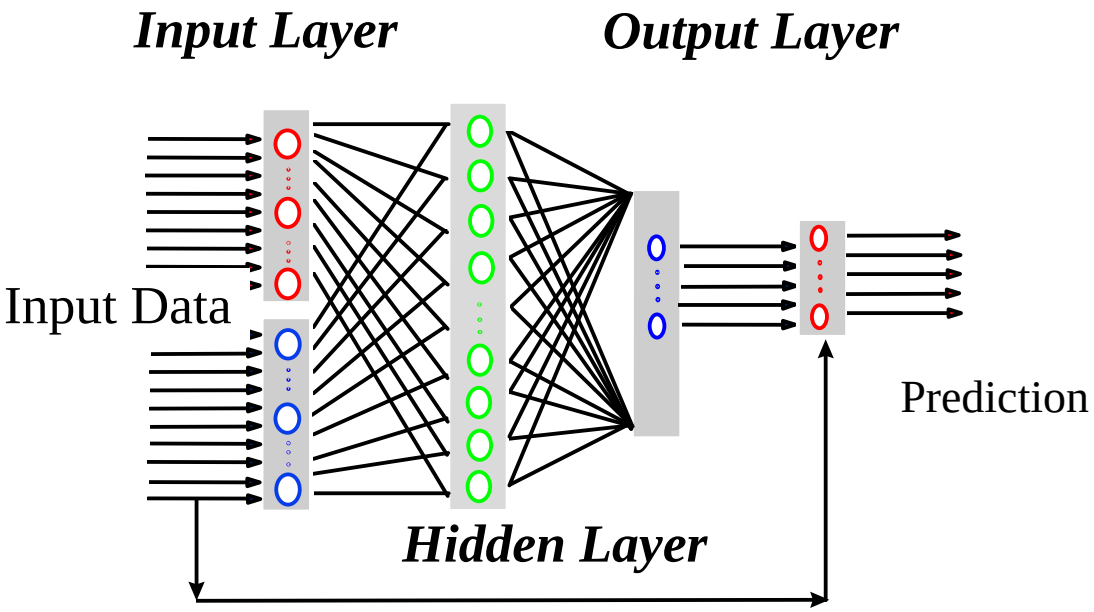

Fig. 21. Non-conventional neural network structure [9, 10].

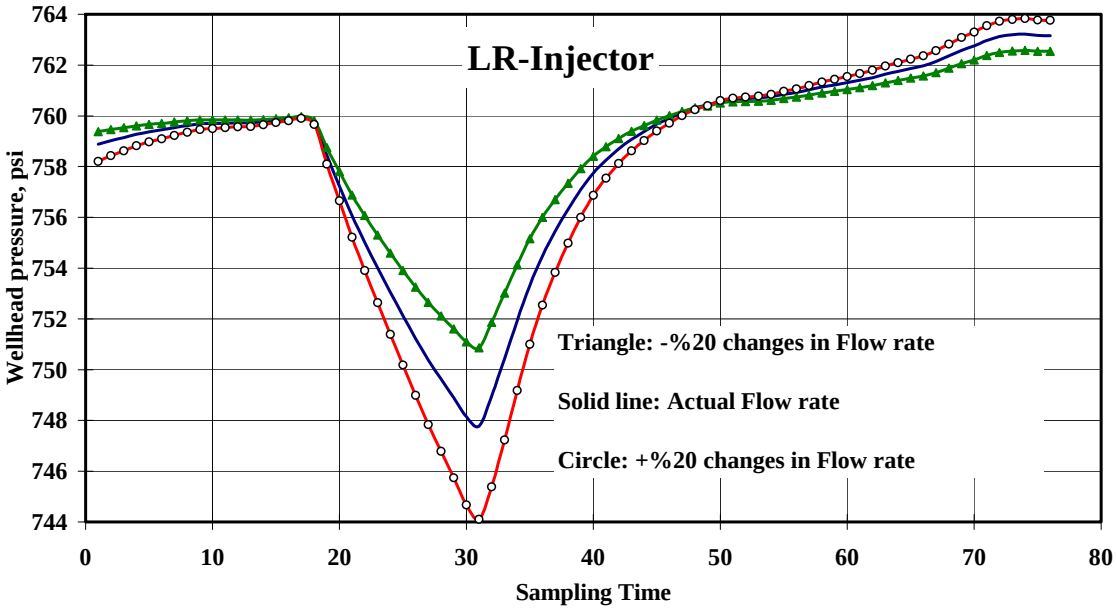

Fig. 22. Open-loop step responses for a series of changes in injection flow rate.

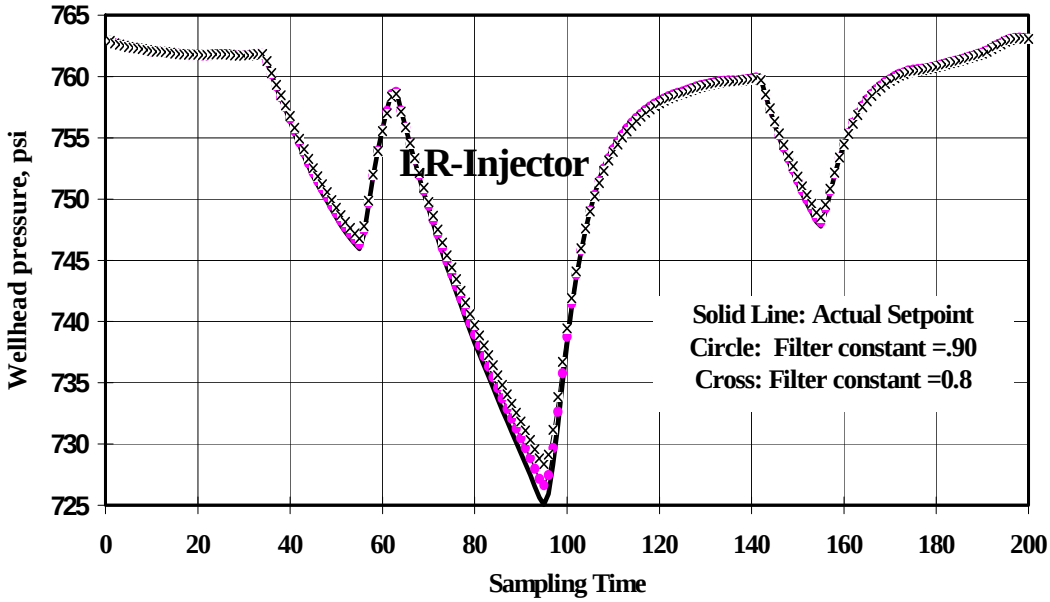

Fig. 23. Setpoint tracking performance of NMPC.